Journal of
Applied Crystallography
ISSN 0021-8898

Received 15 August 2006
Accepted 22 December 2006

Complexity of silicate/aluminosilicate polymerization: some insights using a small-angle X-ray scattering study

Puyam S. Singh

RO Division, Central Salt and Marine Chemicals Research Institute, Bhavnagar 364002, India. Correspondence e-mail: puyam@csmcri.org

The small-angle X-ray scattering study reported here is on growth processes of particles that occurred during silicate/aluminosilicate polymerization starting from clear or colloidal solutions. Two polymerization reaction systems starting from clear homogeneous solutions of silicate monomers or oligomers, and two other polymerization reaction systems starting from silica colloidal solutions, were performed. Early growth of clearly defined silicate particles from a clear solution system was observed, whereas the scattering contrast of early growth processes from another clear system was close to that of the mother liquor and its weak scattering resulted from loosely aggregated structures. In the case of a colloidal solution system, the growth of silica particles was observed from the initial size of the silica nanoparticle reactant by reaction with aluminate anions on its surface, whereas in another colloidal system, depolymerization of the initial silica nanoparticle reactant into smaller silicate units and subsequently polymerization of the smaller silicate units with aluminate anions in solution was observed.

1. Introduction

Inorganic silicate polymerization (Iler, 1979), except the silica in molten glasses, is quite different from the condensation polymerization theory of organic systems. In this inorganic system, three kinds of polymerization stages are generally recognized. They are (i) initial condensation reaction of a monomer to form larger particles; (ii) subsequent growth of the particles; and (iii) aggregation of the particles by linking together into branched chains and networks, forming viscous sols and gels. In the polymerization, there is a strong tendency to form a maximum number of siloxane bonds (–Si—O—Si–) and a minimum of terminal Si—OH groups, and the polymerization quickly leads to ring structures, which are then linked together to form larger three-dimensional structures. These large structures condense internally to the most compact state with terminal Si—OH groups remaining on the outside, resulting in spherical 'nanometer-sized' particles. Dense or hollow spherical silica particles result depending on the reaction conditions of synthesis (Singh & Kosuge, 1998, 2001; Kosuge & Singh, 2001). The polymerization mechanism (Iler, 1979; Okkerse, 1970) involves the formation of either anionic complexes (> pH 2) or cationic complexes (< pH 2). The polymerization process starting from the early nuclei to stable colloid is well studied by the small-angle X-ray scattering (SAXS) technique because SAXS is an excellent tool to characterize the size and shape of nanoparticles (Guinier & Fournet, 1955). The nucleation and growth of crystalline silicalite (only silicate network) and aluminosilicate zeolites were well studied by SAXS data from the early stages of polymerization processes (Watson *et al.*, 1997; de Moor *et al.*, 1997; Singh *et al.*, 1999; Singh & White, 1999). The silica nanoparticles prepared by the Stöber method (Stöber *et al.*, 1968) using ammonia and TEOS (tetraethylorthosilicate) were best characterized by SAXS (Boukari *et al.*, 1997) and ultra-SAXS (Boukari *et al.*, 2000). In these studies, the first detected particles in the solution have R_g (radius of gyration) of about 10 nm, and these initial 10 nm radii particles are of low density and form aggregated structures by mutual interactions among the particles. Smooth, dense particles are only observed in a later stage by the densification of the initial low-density particles. Using time-resolved synchrotron SAXS (Pontoni *et al.*, 2002), the very early stages of particle nucleation from solution were investigated and the result was consistent with the above aggregation process involving primary particles of about 10 nm radii. Growth of small particles (1–10 nm) from the solution of this system was not detected. The silica nanoparticles prepared from another method using an acid-catalysed system of TEOS: $6.4H_2O$:$3.8C_2H_5OH$:$0.085HNO_3$ had also been investigated by SAXS (de Lange *et al.*, 1995). In this case, the first detected primary 'low-density' particles in the solution have R_g of about 2 nm, and later grow to denser particles of about 4 nm radii.

In the present paper, we report a SAXS study of 'silicate/aluminosilicate particle growth processes occurred from four different systems that have clear or colloidal starting solutions'. The clear solution systems are from starting solutions of either TEOS monomers or oligomeric silicate anions, while the colloidal solution systems are from 10 nm-sized silica particles.

2. Experimental

2.1. Materials synthesis

System I. An appropriate amount of TEOS was dissolved in an ethanol–water mixture containing a small amount of HCl. A few solution mixtures of different TEOS content were prepared and their

molar compositions are in the range 0.1–1TEOS:1000H_2O: 100C_2H_5OH: 3HCl. For comparison, another sample was prepared with an excess amount of HCl (1TEOS:1000H_2O:100C_2H_5OH:9HCl). A water-soluble polymer dispersant, such as polyethylene glycol or polyvinylalcohol (25–75 wt%), was added to the above mixture. The added polymer dispersant was to reduce agglomeration of particles during the polymerization process of silica.

System II. Appropriate amounts of aluminium wire and fumed silica were dissolved separately in aqueous sodium hydroxide solutions. Both solutions were filtered through 0.2 μm Millex filters and the filtered solutions were then mixed together. The resultant solution was clear and homogeneous and had a molar composition of 9Na_2O:0.15Al_2O_3:1SiO_2:200H_2O.

System III. Ludox SM-30 (30 wt% suspension in water) colloidal silica was mixed with aluminate anions formed by the reaction of polymeric aluminium hydroxide with TMAOH (tetramethylammonium hydroxide) and NaOH. A few solution mixtures having different alkali content were prepared and their molar compositions were in the range 0.2–2Na_2O:1Al_2O_3:3.4SiO_2:2$(TMA)_2O$:370H_2O.

System IV. Ludox SM-30 (30 wt% suspension in water) colloidal silica was mixed with aluminium anions formed by the reaction of monomeric aluminium isopropoxide with TMAOH and NaOH. This system had a starting mixture of composition 0.05Na_2O:1Al_2O_3: 2SiO_2:2.5$(TMA)_2O$:127H_2O.

2.2. SAXS data analysis

The SAXS measurements were taken at room temperature or higher using an X-ray beam of wavelength 1.54 Å (Cu $K\alpha$) and the smallest modulus of scattering vector (Q) achievable was about 0.01 Å. The scattering intensity is given by the general equation

$$I(Q) \propto P(Q)\,S(Q). \quad (1)$$

Q is defined as $Q = (4\pi/\lambda)\sin\theta$, where λ is the wavelength and 2θ is scattering angle. The form factor $P(Q)$ reflects the distribution of scattering material in the scattering particle, and the structure factor $S(Q)$ is related to the spatial distribution of the scattering particles in the surrounding medium such as solvent.

The scattering data are fitted for a population of polydisperse spheres, including structure factor arising from hard sphere interactions between the particles using the Percus–Yevick closure and a Schulz distribution.

3. Results and discussion

3.1. Clear solution systems

3.1.1. System I. Fig. 1 shows the SAXS profile [$I(Q)$ *versus* Q] over the Q range 0.014–0.2 Å^{-1} from three samples of this system having different amounts of TEOS (samples 01, 02, 03), measured after reacting the mixture at room temperature for about 2 d, along with the scattering profile of sample 04, which was made with excess HCl (three times the amount used in the other samples) at the same reaction condition. Scattering from the samples was good and fitted for a population of polydisperse spheres, including structure factors arising from interactions between the particles. The scattering data from samples 01, 02 and 03 over the Q range 0.02–0.15 Å^{-1} is fitted well with polydisperse spheres with median sphere radii 4.0, 3.7 and 3.7 nm, respectively, and the decrease in scattering intensity over the lower Q range 0.014–0.03 Å^{-1} is in agreement with the interaction between the particles forming some aggregated particles of about 11 nm radii. In the scattering profile of sample 04, there is a relatively very high intensity and steep curve at the lower Q range (0.014–0.03 Å^{-1}), and the scattering profile over the higher Q range (0.03–0.15 Å^{-1}) almost matches those of other samples. This suggests that some larger polydisperse particles, at least larger than those aggregated particles of samples 01, 02 and 03, along with smaller particles of about 4 nm radii were being concurrently formed in sample 04.

The polymerization of TEOS on reaction with water involves both hydrolysis and condensation reactions. Polymeric silica is a cross-linked silicate network and generally comprises $Si(OSi)(OH)_3$, $Si(OSi)_2(OH)_2$, $Si(OSi)_3(OH)$ and $Si(OSi)_4$ structural units. It has very little ionic charge and therefore charge repulsion is insignificant, and thus particles can collide and aggregate into chains and continuous networks. The relative reaction rates of hydrolysis and condensation may be related to the formation of polydispersed low- or high-density particles. The aggregated particles, as a result of interaction between the nanoparticles, were found to be present in all of the samples, and there was maximum degree of aggregation as a result of rapid hydrolysis and condensation reactions in sample 04 prepared with excess HCl.

3.1.2. System II. The solution mixture in this system is dissolved silicate and aluminate anions in highly alkaline environment. The silicate anions may consist of a range of oligomeric structures. However, their sizes are at least smaller than 1 nm as evident from the structures given by NMR studies (Engelhardt & Michel, 1987). The SAXS patterns for the solution mixture at ambient temperature over the period of 1–10 h were measured to check the polymerization reactions. The scattering is weak and no scattering signatures of specific forms were observed from the solution mixture even after the exposure of 10 h. The scattering profile of the solution mixture is plotted in Fig. 2. The scattering profile, however, exhibits power law behaviour, which suggests that some degree of aggregation takes place when the solution mixture is reacted at room temperature and the X-ray scattering length density of these aggregated particles (ρ_3) is close to that of the surrounding medium, which is the sum of the scattering density of water (ρ_1) and the inorganic anions (ρ_2). The

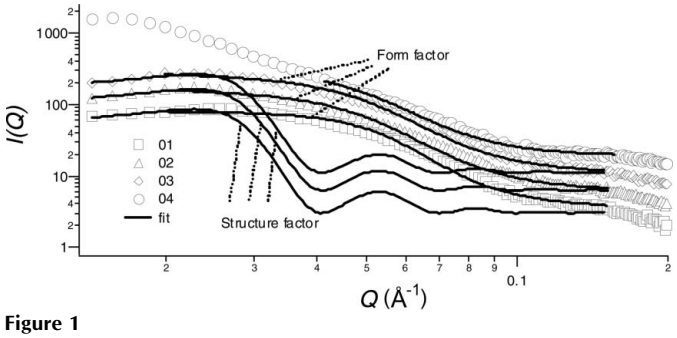

Figure 1
Small-angle X-ray scattering from the samples (01 to 04) of system I over the 0.015–0.2 Å^{-1} Q range.

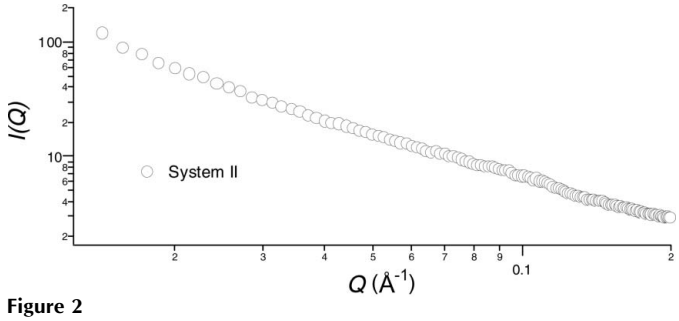

Figure 2
SAXS profile of the solution mixture from system II at ambient temperature after exposure of 10 h.

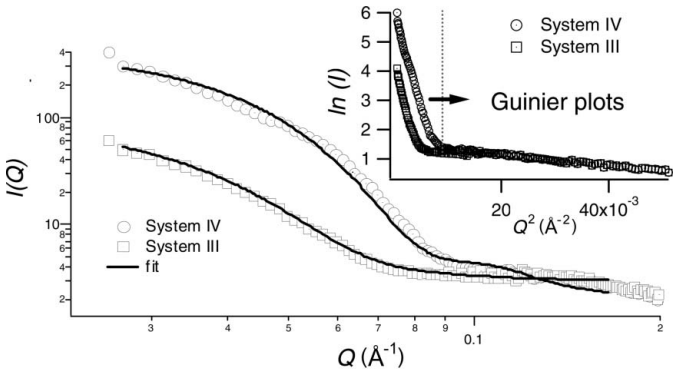

Figure 3
SAXS patterns from the initial solution mixtures of system III and IV. Guinier plots are given in inset.

aggregation process may be due to formation of aluminosilicate structures *via* Al—O—Si bond linkages. This is quite likely because self-aggregation of silicate anions is not possible under such highly alkaline systems.

3.2. Colloidal solution systems

SAXS patterns of initial solution mixtures of systems III and IV are shown in Fig. 3. Fits to the SAXS curves as well as Guinier plots (inset of Fig. 3) indicate that both the solution mixtures consist of well dispersed, uniform colloidal particles of 10 nm in diameter. However, the scattering contrast (difference between scattering densities of particles and surrounding medium) of the solution mixture of system III is much lower than the scattering contrast of the system IV solution mixture, and the scattering contrast of the system IV solution is quite close to the scattering contrast of colloidal silica in water. This indicates that either the scattering density of the colloidal silica particle is lowered or the scattering density of the surrounding medium is increased in the initial solution mixture of system III compared with that of system IV.

3.2.1. System III. In this case, the colloidal silica was mixed with aluminate anions formed by the reaction of polymeric aluminium hydroxide with TMAOH and NaOH. The scattering patterns were taken from the samples after reacting at elevated temperatures for different reaction times or by changing the alkali content. In a low-NaOH solution system the particle diameter was 10 nm, whereas in a high-NaOH system the particle diameter, determined from the Guinier radius and form factor fit, was 13 nm. In a very high NaOH system the solution becomes a viscous gel. A change in colloidal particle size was also seen with polymerization reaction time. These are schematically presented in Fig. 4. The change in radius of the spheres is almost exactly what would be expected to produce the change in scattering intensity. The change in scattering intensity [$I(0)$, from Guinier extrapolation] in this case is proportional to the sixth power of the radius, exactly what would be expected for homogeneous growth. The log–log plot of 'intensity' *versus* 'radius' of the experimental results exactly matches the theoretical plot, as shown in Fig. 4 (inset).

3.2.2. System IV. Here, the NaOH content of the reaction mixture was at least four times lower than the amount used in the system III solution; secondly the aluminate anions were formed by the reaction of monomeric aluminium isopropoxide with TMAOH and NaOH. In this solution system, the initial particle size gradually decreases from 10 to 9 nm. The data can be interpreted on the basis that the silica particles are partially dissolved by the action of the alkali present in the solution. The schematic representation of the polymerization process is shown in Fig. 5. In this period, the scattering intensity, $I(0)$ decreases very much more than the expected intensity. The experimental and theoretical log–log plots of 'intensity' *versus* 'radius' are also shown in Fig. 5. This incompatibility on the basis of number, size and density suggests that the scattering contrast is further reduced by increased scattering density of the surrounding medium. The increased scattering density of the surrounding medium can be derived from the additional scattering density of newly formed small particles in solution.

These observations suggest that for synthesis system III the polymerization of silica colloid with aluminate anions is in the solid state initially at the surface of the silica spheres, but proceeds inwards as the reaction progresses. In the case of synthesis system IV, the polymerization process is first by dissolving silica spheres, and then

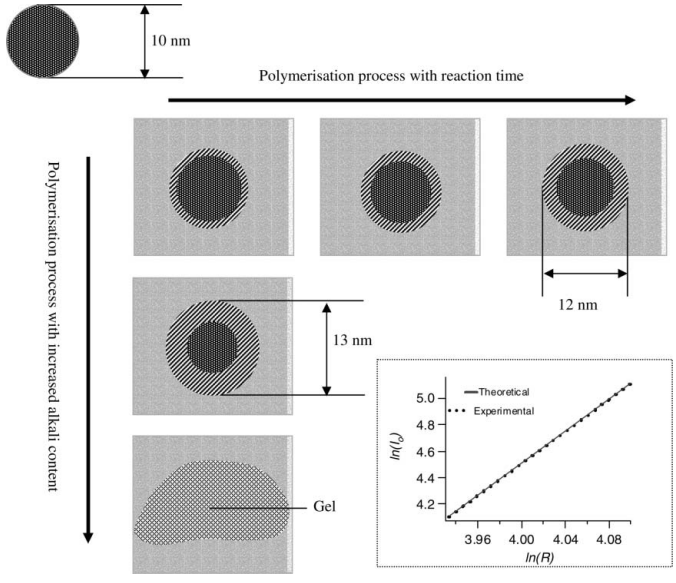

Figure 4
Schematic representation of polymerization processes of system III reaction mixtures. Inset: log–log plot of 'intensity' *versus* 'radius'

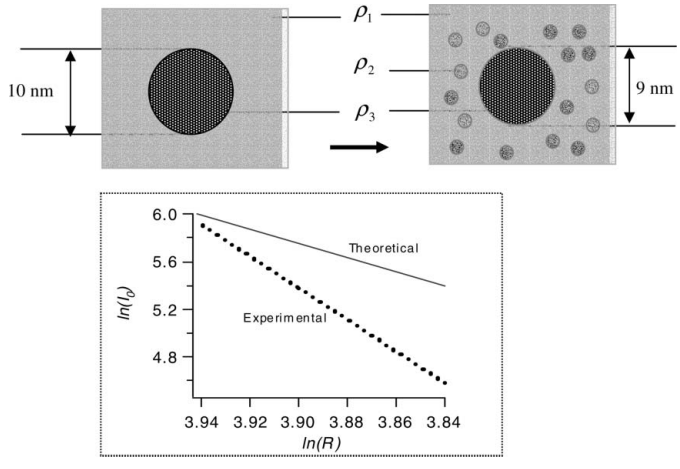

Figure 5
Top: Schematic representation of polymerization processes of system III reaction mixtures. Bottom: log–log plot of 'intensity' *versus* 'radius'.

reacting the dissolved silicate anions with aluminate anions in solution.

4. Conclusion

The growth processes of particles that occurred during silicate/aluminosilicate polymerizations starting from clear or colloidal solutions were examined by small-angle X-ray scattering. The clear solution (system I) preparation showed the growth of silica particles of ~4 nm radii from organosilicate monomers. A high degree of aggregation or clustering of particles leading to bigger particle was clearly observed in the case where hydrolysis and condensation reactions were not better controlled. In the case of a clear and highly alkaline solution system (system II) containing dissolved silicate anions and aluminate anions, the polymerization reaction is slow and only loosely aggregated aluminosilicate structures are formed. In colloidal solution system III the initial silica particles of 10 nm in diameter transform to larger aluminosilicate particles by the reaction of aluminate anions on its surface, and the polymerization process appears to be a continuous and homogeneous one. In the case of colloidal solution system IV, the transformation process involves a reduction in the diameter of the initial silica particles (10 nm) by partial dissolution in solution and the polymerization of dissolved silicate species with aluminate anions in solution.

The author is very grateful to Dr P. K. Ghosh, Director, CSMCRI (CSIR) for encouragement and partial financial assistance to attend the XIII International Conference on Small-Angle Scattering. The financial support for travel and registration fee from the Conference Organizing Committee is also gratefully acknowledged.

References

Boukari, H., Lin, J. S. & Harris, M. T. (1997). *J. Colloid Inteface Sci.* **194**, 311–318.
Boukari, H., Long, G. G. & Harris, M. T. (2000). *J. Colloid Inteface Sci.* **229**, 129–139.
Engelhardt, G. & Michel. D. (1987). *High-Resolution Solid-State NMR of Silicates and Zeolites*. New York: John Wiley and Sons Ltd.
Guinier, A. & Fournet, G. (1955). *Small Angle Scattering of X-rays*. New York: John Wiley and Sons Ltd.
Iler, R. K. (1979). *Chemistry of Silica*. New York: John Wiley and Sons Ltd.
Kosuge, K. & Singh, P. S. (2001). *Chem. Mater.* **13**, 2476–2482.
Lange, R. S. A. de, Hekkink J. H. A., Keizer, K. & Burggraff, A. J. (1995). *J. Non-crystalline Solids*, **191**, 1–16.
Moor, P. E. A. de, Beelen, T. P. M., Komanschek, B. U., Diat, O. & van Santen, R. A. (1997). *J. Phys. Chem. B*, **101**, 11077–11086.
Okkerse, C. (1970). *Porous Silica* in *Physical and Chemical Aspects of Adsorbents and Catalysts*, edited by B. G. Linsen, p. 219. New York: Academic Press.
Pontoni, D., Narayanan, T. & Rennie, A. R. (2002). *Langmuir*, **18**, 56–59.
Singh, P. S., Dowling, T. L., Watson, J. N. & White, J. W. (1999). *Phys. Chem. Chem. Phys.* **1**, 4125–4130.
Singh, P. S. & Kosuge, K. (1998). *Chem. Lett.* **1**, 63–64.
Singh, P. S. & Kosuge, K. (2001). *Microporous Mesoporous Mater.* **44**, 139–145.
Singh, P. S. & White, J. W. (1999). *Phys. Chem. Chem. Phys.* **1**, 4131–4138.
Stöber, W., Fink, A. & Bohn, E. (1968). *J. Colloid Inteface Sci.* **26**, 62–69.
Watson, J. N., Iton, L. E., Keir, R. I., Thomas, J. C., Dowling, T. L. & White, J. W. (1997). *J. Phys. Chem. B*, **101**, 10094–10104.